J Supercond Nov Magn (2017) 30:1515–1525
DOI 10.1007/s10948-016-3946-8

ORIGINAL PAPER

Effect of Monovalent Cation Doping on Structural, Magnetic, and Magnetocaloric Properties of $Pr_{0.85}A_{0.15}MnO_3$ (A = Ag and K) Manganites

Gönül Akça[1] · Ali Osman Ayaş[2] · Selda Kılıç Çetin[1] · Mustafa Akyol[1] · Ahmet Ekicibil[1]

Received: 23 June 2016 / Accepted: 29 November 2016 / Published online: 13 December 2016

Abstract A systematic study on the effect of monovalent cation doping on structural, magnetic, and magnetocaloric properties of $Pr_{0.85}A_{0.15}MnO_3$ (A = Ag and K) samples synthesized by a sol-gel method has been carried out. The crystal structure and morphology have been worked by X-ray diffraction (XRD) and scanning electron microscopy (SEM) imaging measurements. The XRD results indicate that both samples have orthorhombic structure. Magnetization versus temperature measurements show that our samples display a ferromagnetic-to-paramagnetic phase transition with increasing temperature. The ferromagnetic-to-paramagnetic phase transition temperature (T_C) values were found as 74 and 116 K for $Pr_{0.85}Ag_{0.15}MnO_3$ and $Pr_{0.85}K_{0.15}MnO_3$, respectively. The magnetic entropy changes were evaluated from isothermal magnetization curves measured at various temperatures near T_C by steps of 4 K. The values of the magnetic entropy change were determined as 0.99 and 1.39 J kg^{-1} K^{-1} for $Pr_{0.85}Ag_{0.15}MnO_3$ and $Pr_{0.85}K_{0.15}MnO_3$ under external field changes of 10 kOe, respectively.

Keywords Manganites · Magnetic properties · Magnetic entropy change · Magnetocaloric effect

✉ Ali Osman Ayaş
aayas@adiyaman.edu.tr

[1] Department of Physics, Faculty of Sciences and Letters, Çukurova University, 01330 Adana, Turkey

[2] Department of Mechatronics Engineering, Faculty of Technology, Adıyaman University, 02040 Adıyaman, Turkey

1 Introduction

The magnetocaloric effect (MCE), described as cooling or heating of a magnetic material under magnetic field change, offers an alternative technology for refrigeration [1]. The magnetic refrigeration (MR) technology has basic advantages over a classical system such as not emitting environmentally harmful gases and being more energy efficient [2–4]. It would be possible to achieve mentioned advantages only if desired magnetic materials can be produced. For this reason, MCE has been investigated widely to find a proper refrigerant material that can produce large entropy change when it goes through magnetization-demagnetization process [5–7]. So far, it has been reported that the large spontaneous magnetization and a sharp change in the magnetization with changing temperature are important requirements for magnetic material to possess large magnetic entropy change [8, 9]. The perovskite manganites having the general formula $RE_{1-x}A_xMnO_3$ (RE and A are a trivalent rare-earth cation and a divalent or monovalent cation, respectively) have attracted much attention due to their interesting physical and magnetic properties such as colossal magnetoresistance (CMR) and MCE [10–12]. It is known that $REMnO_3$ is an antiferromagnetic insulator [13]. The magnetic and transport properties of these base samples are strongly affected by the percentage of the divalent or monovalent cation ions, the ionic radii of these ions, and the preparation method of the samples [14, 15]. For RE = Pr case, in the literature, there are a lot of studies about the structural, magnetic, and magnetocaloric properties with divalent substitutions. However, the substitution of monovalent (A = Na, K, Ag, etc.) elements by RE ions has been much less studied [13, 16–21]. Jirák et al. reported structural and physical properties of $Pr_{1-x}A_xMnO_3$ manganites $0 \leq x \leq 0.15$ for K [16] and $0 \leq x \leq 0.2$ for Na [17],

respectively. According to their studies, the optimum doping level is determined as 0.15 for the substitution of monovalent cation in $PrMnO_3$ [18]. In the present work, we have explored the effect of the monovalent cation substitution on structural, magnetic, and magnetocaloric properties in $Pr_{0.85}A_{0.15}MnO_3$ (A = Ag and K) manganites. The percentage of the monovalent cations has the same ratio for both samples.

2 Experimental Procedure

We have prepared polycrystalline $Pr_{0.85}A_{0.15}MnO_3$ for A = Ag and K samples, labeled as PAM and PKM, respectively. The sol-gel method was used to obtain high-purity and homogenous powder samples. An appropriate amount of $Pr(NO_3)_3{\cdot}6H_2O$, MnO_2, $AgNO_3$, and KNO_3 powders was liquefied in suitable diluents to obtain desired stoichiometry for PAM and PKM samples. We used 87.91 g (five times of the total mole number of main compound) citric acid monohydrate (CAS number: 5949-29-1) with $\geq$99.95 % purity and 23.38 cm^3 (five times of the total mole number of main compound) mono-ethylene glycol with 99.8 % purity (CAS number: 107-21-1) as reagents and solvents, respectively. Then, the solution was stirred at 300 °C until dry gel was formed. The dry gel was first burned at 500 °C for an hour and then calcined at 550 °C for 5 h so that organic substances will be removed from the materials. To get fine powders, the materials were ground by using an agate mortar. After that, the microcrystalline powder was pressed into disks and sintered at 970 and 1150 °C during 24 h for PAM and PKM, respectively. The crystal structure of the powder samples was identified by X-ray diffraction (XRD) using Cu K_α radiation. The microstructural properties and elemental analysis of the samples were investigated by scanning electron microscopy (SEM) combined with energy-dispersive X-ray spectroscopy (EDS). Magnetic measurements were performed by using a vibrating sample magnetometer (VSM). The magnetic entropy changes (ΔS_M) were obtained from isothermal magnetization curves which were taken up to 1 T at various temperatures near T_C by intervals of 4 K.

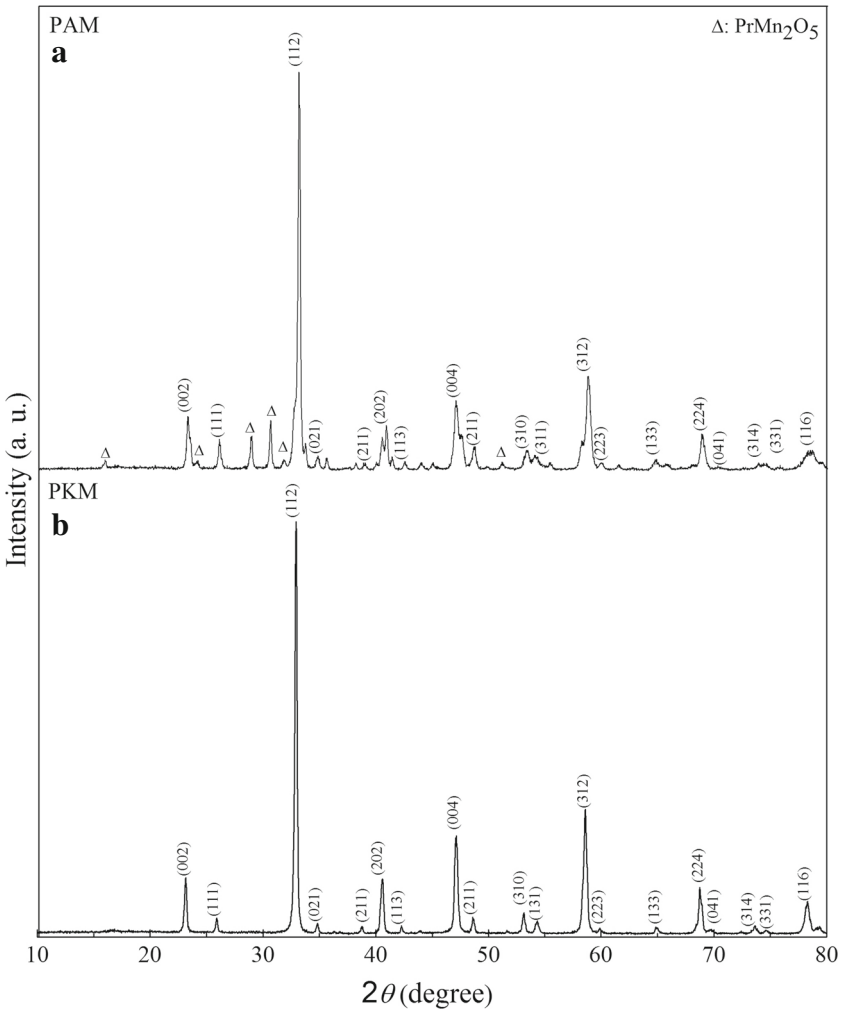

Fig. 1 The XRD patterns of the $Pr_{0.85}A_{0.15}MnO_3$ *a* PAM and *b* PKM samples

Table 1 The lattice parameters, unit cell volume, A site average ionic radius ($\langle r_A \rangle$), and tolerance factor (t_f) of the PAM and PKM samples

Sample codes	a (Å)	b (Å)	c (Å)	V (Å^3)	$\langle r_A \rangle$ (Å)	t_f
PAM	5.435	5.490	7.670	228.858	1.1491	0.8935
PKM	5.439	5.485	7.724	230.429	1.1836	0.9087

3 Results and Discussions

Figure 1 shows the X-ray diffraction patterns recorded at room temperature using Cu K_α radiation for $Pr_{0.85}A_{0.15}MnO_3$ (A = Ag and K) samples. It can be seen from the figure that both samples have been crystallized as perovskite structure. The peaks become larger and narrower which indicate better crystallization in the PKM than in the PAM sample. The XRD patterns of the PAM and PKM samples are indexed in the orthorhombic structure with a *Pbnm* space group by using PANalytical X'Pert HighScore Plus software. From Fig. 1, the PAM sample has a small amount of impurity phases (4.90 % of the compound) related to the presence of $PrMn_2O_5$ symbolized by a triangle. We believed that the presence of this impurity phase does not affect the observed magnetocaloric behavior of the sample since it is non-ferromagnetic impurity [22]. The lattice parameters of samples are obtained as $a = 5.435$ Å, $b = 5.490$ Å, and $c = 7.670$ Å for PAM and $a = 5.439$ Å, $b = 5.485$ Å, and $c = 7.724$ Å for PKM from the XRD data. The unit cell volumes of the samples are found as 228.858 and 230.429 Å^3 for PAM and PKM samples, respectively. It is seen that there is a slight difference in the value of lattice parameters and the unit volume of samples. The average crystallite sizes, calculated from the Scherrer relation [23], are found as 38 and 56 nm for PAM and PKM, respectively. The average crystallite size of PKM is obviously bigger than that of PAM. The reason of differences of lattice parameters and crystallite sizes between PAM and PKM might be related to having larger ionic radii of K (1.51 Å) than Ag (1.28 Å) [24] The lattice distortion can be estimated by a tolerance factor formulated as $t_f = (r_A + r_O) \Big/ \sqrt{2}\,(r_{Mn} + r_O)$ where r_A, r_{Mn}, and r_O are the ionic radii of A site, Mn site, and oxygen ion, respectively [25]. The A site average ionic size ($\langle r_A \rangle$) and the tolerance factor (t_f) of samples were calculated using values of ionic radii by Shannon for coordination number 8 for the A site cations and coordination number 12 for oxygen [24]. The values of the $\langle r_A \rangle$ and the t_f are given in Table 1. The value of the $\langle r_A \rangle$ for the PKM sample is bigger than that of the PAM due to having a bigger ionic radius of K than Ag. The t_f value of both samples is in the constant range of perovskite structure [26]. Figure 2a, b shows the SEM images and EDS spectra for PAM and PKM samples, respectively. It is seen from the SEM images that each sample is formed in different shape grains. The average grain sizes of the samples, calculated from 100 arbitrary grains, are found as 0.71 and 0.94 μm for PAM and PKM samples, respectively. The average grain sizes are larger than those calculated from the XRD data. It is evident that the grains are formed from several crystallites [27]. It is seen from the EDS spectra that the samples contain all of the expected elements and any impurity element has not been identified.

In order to determine the magnetic behavior of the samples, we have performed the temperature $M(T)$ and applied magnetic field $M(H)$ dependence of the magnetization measurements. $M(T)$ curves of both samples measured in zero-field-cooled (ZFC) procedure at a magnetic field of 250 Oe are shown in Fig. 3a, b. It can be seen that magnetization increases by increasing the temperature from 10 K to the magnetic phase transition point, which depends on doping of K or Ag elements. This behavior may have arisen due to the suppression of magnetization caused by the coexistence of ferromagnetic/antiferromagnetic couplings and/or spin glass that yields to an anisotropic field inside the samples [28–31]. When the temperature is even increased, the magnetization starts to decrease which indicate a ferromagnetic-to-paramagnetic phase transition at temperature (T_C). From the minimum point of the $dM/dT - T$ curve given as an inset graph in Fig. 3a, b, the T_C values of samples were determined as 74 and 116 K for PAM and PKM samples, respectively (Table 2). The small ionic radius of Ag with respect to the K causes the decrease of the $\langle r_A \rangle$. This decrease leads to a change in Mn–O–Mn bond angle and Mn–O length. Therefore, a double-exchange interaction might be weaker because of the changing of bandwidth and mobility of e_g electrons [32, 33] and, consequently, the Curie temperature value of the samples decreases from 116 to 74 K by changing K with Ag [28]. It can be seen from Fig. 3a, b that the phase transition becomes sharper by changing Ag with K and this situation supports the former explanations given above as well. Figure 3a, b also displays the temperature dependence of the inverse magnetic susceptibility, $1/\chi - T$. At high temperature region, they show a linear behavior corresponding with paramagnetic state. By fitting the inverse susceptibility data with the Curie-Weiss law given by $\chi = C/(T - \theta)$, where C is the Curie constant and θ is the paramagnetic Curie temperature, we have determined the θ value as 81 and 117 K for Ag and K, respectively. The θ value is nearly in accordance with T_C for the PKM sample. However, for the PAM sample, the θ value is higher than T_C, which might be related to the magnetic inhomogeneity and impurity [34]. The Curie constant is given by $C = \frac{N\mu_{eff}^2\mu_B^2}{3k_B}$ where N is Avogadro's number, μ_B is the Bohr magneton, μ_{eff} is the effective magnetic moment, and k_B is the Boltzmann constant. The Curie constant values of the samples are calculated from

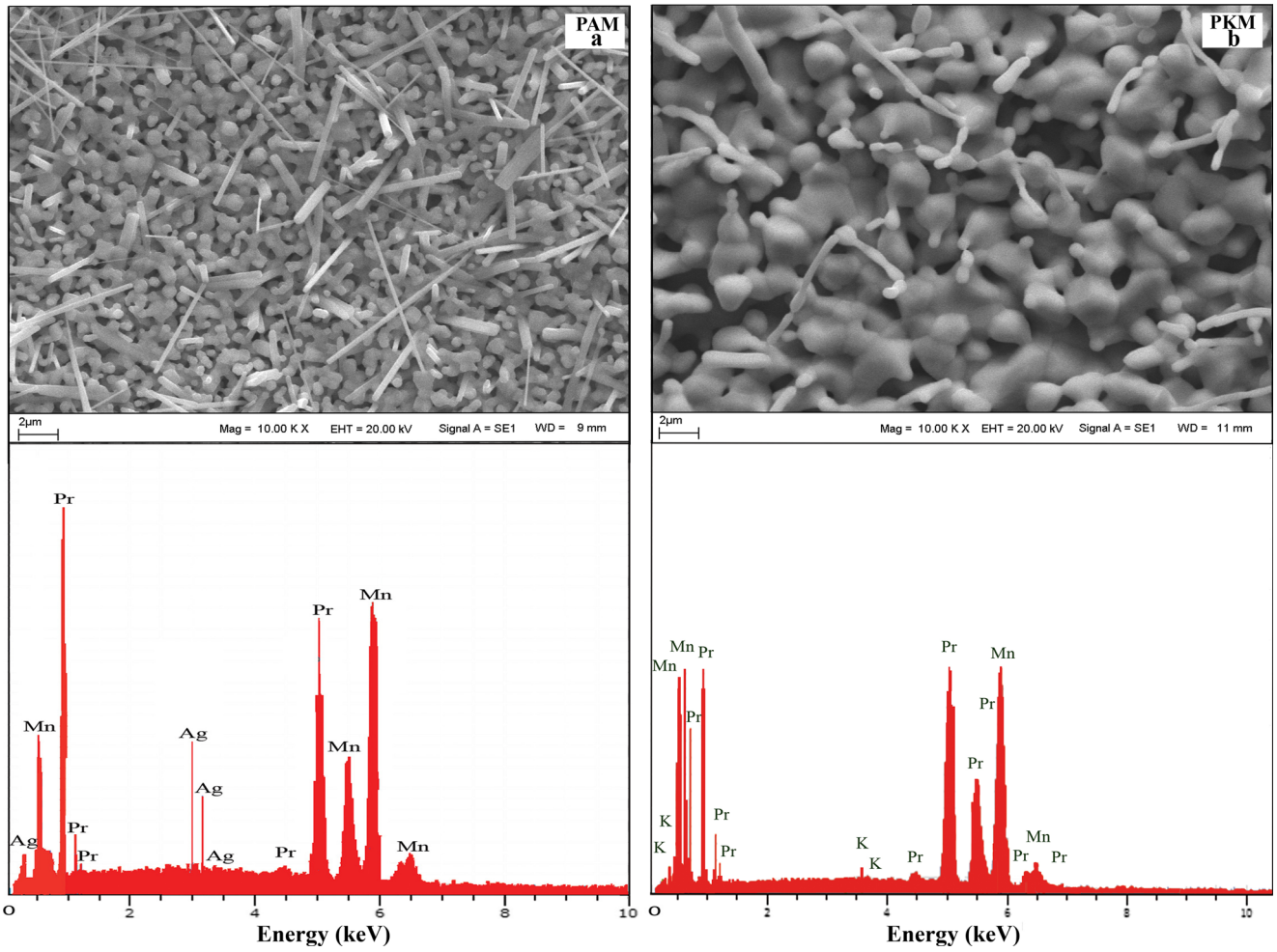

Fig. 2 The SEM images and EDS spectra of the $Pr_{0.85}A_{0.15}MnO_3$ samples **a** PAM and **b** PKM

the slopes of $1/\chi - T$ curves. By using these values, μ_{eff} values were determined as 3.43 μ_B and 3.99 μ_B, for PAM and PKM, respectively. These values are smaller than theoretically estimated effective magnetic moment value ($\mu_{\text{eff}}^{\text{cal}}$, 4.61 μ_B), which indicates the canted situation of the spin ordering [35–37]. Figure 4a, b represents the magnetic field dependence of magnetization curves, $M(H)$, measured in the vicinity of transition temperature for each sample. The $M(H)$ curves of the samples display a nonlinear behavior as a typical ferromagnetic state at $T < T_C$ [38], and then they become linear that shows a paramagnetic behavior above T_C. In the vicinity of T_C, we crossed out H/M versus M^2 (the so-called Arrott plots) to define the type of the magnetic phase transition. The Arrott plots of each sample are shown in Fig. 5a, b. According to the Banerjee criterion, the slope of the H/M versus M^2 curves indicates the order of magnetic phase transition. Since it is well known that the positive (negative) slope of the curve indicates the second (first)-order magnetic phase transition [39], our both PAM and PKM samples show a second-order magnetic phase transition due to the positive slope of their Arrott plots.

From isothermal $M(H)$ measurements, the magnetic entropy change (ΔS_M) has been determined using the classical thermodynamic theory based on Maxwell's relation [40]

$$-\Delta S_M(T, H) = \sum_i \frac{M_i - M_{i+1}}{T_{i+1} - T_i} \Delta H_i \quad (1)$$

Table 2 The summary of magnetic and magnetocaloric properties of $Pr_{0.85}A_{0.15}MnO_3$ (A = Ag and K) manganites

Sample codes	T_C (K)	θ (K)	μ_{eff} (μ_B)	RCP (J kg^{-1}) (1 T)	$-\Delta S_M^{\max}$ (J kg^{-1} K^{-1}) (1 T)
PAM	74	81	3.43	35.6	0.99
PKM	116	117	3.99	33.7	1.39

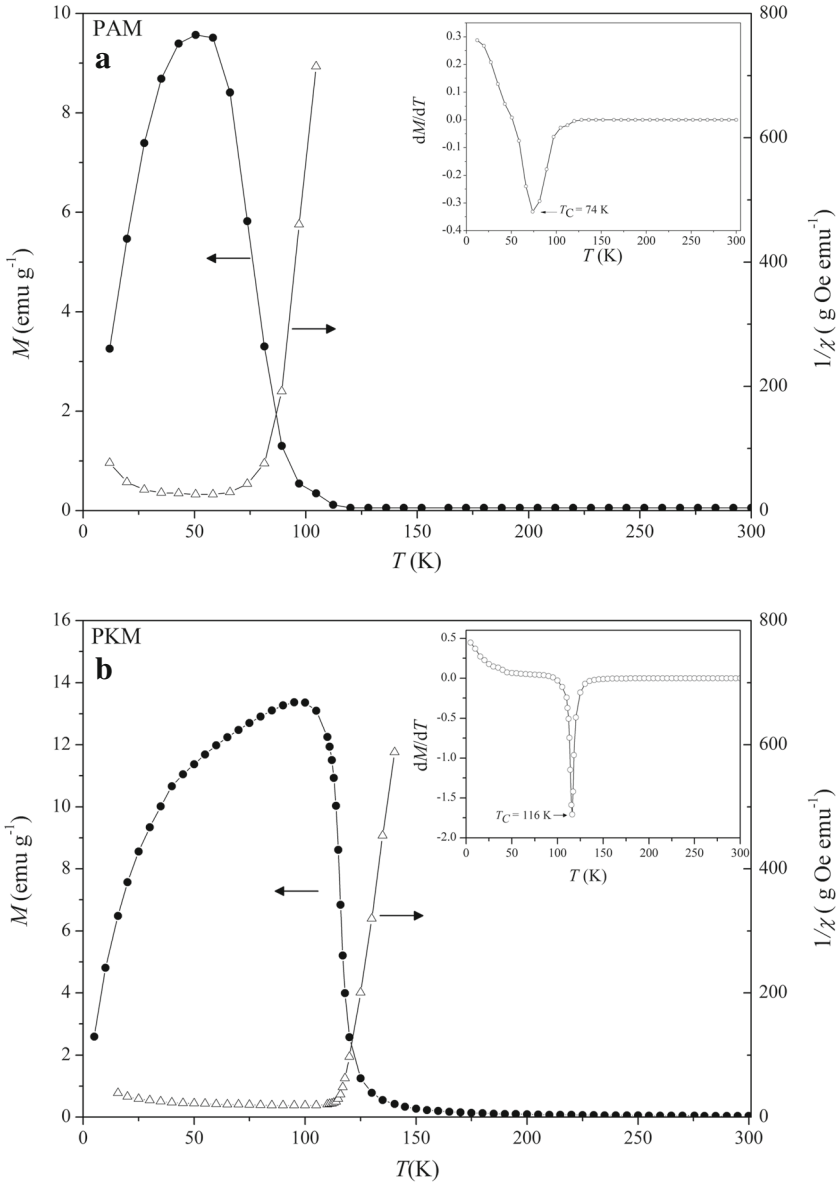

Fig. 3 M(T) and inverse susceptibility for the (a)PAM, (b) PKM samples at 25 mT applied magnetic field. Left axes: temperature dependence of magnetization. Right axes: the temperature dependence of the D.C. inverse susceptibility. Insets: the temperature dependence of dM/dT

where M_i and M_{i+1} are the experimental values of the magnetization at temperatures T_i and T_{i+1}, respectively, under a magnetic field H_i. Figure 6a, b shows the magnetic entropy change curves as a function of temperature in a magnetic field change of 1 T for PAM and PKM samples. In a magnetocaloric system, the biggest magnetic entropy change occurs around the transition temperature where the magnetization has an abrupt variation. Thus, we have performed isothermal magnetization measurements around T_C. The values of ΔS_M^{max} are found as 0.99 and 1.39 J kg^{-1} K^{-1} for PAM and PKM at $\Delta H = 1$ T, respectively. These results are comparable with the values of monovalent or divalent perovskite manganites [15, 41, 42]. The ΔS_M^{max} value of PKM is obviously larger than that of PAM. The lower ΔS_M^{max} value of the PAM sample might be arisen from (i) the presence of impurity phases that increases the volume fraction of non-magnetocaloric part of PAM and (ii) the broader magnetic phase transition of the PAM sample.

Amaral et al. [43] and Amaral and Amaral [44] focused on more accurate theoretical modeling of MCE that was based on the Landau theory of phase transitions. According to the theory, the magnitude and the temperature dependence of the ΔS_M are closely related with magnetoelastic coupling and electron condensation energy. In order to analyze the ΔS_M properties of the sample in accordance with this theory, we have used the Gibbs free energy expressed in the following equation [43, 44]:

$$G(M,T) = G_0 + \frac{A(T)}{2}M^2 + \frac{B(T)}{4}M^4 + \frac{C(T)}{6}M^6 \ldots - \mu_0 H \quad (2)$$

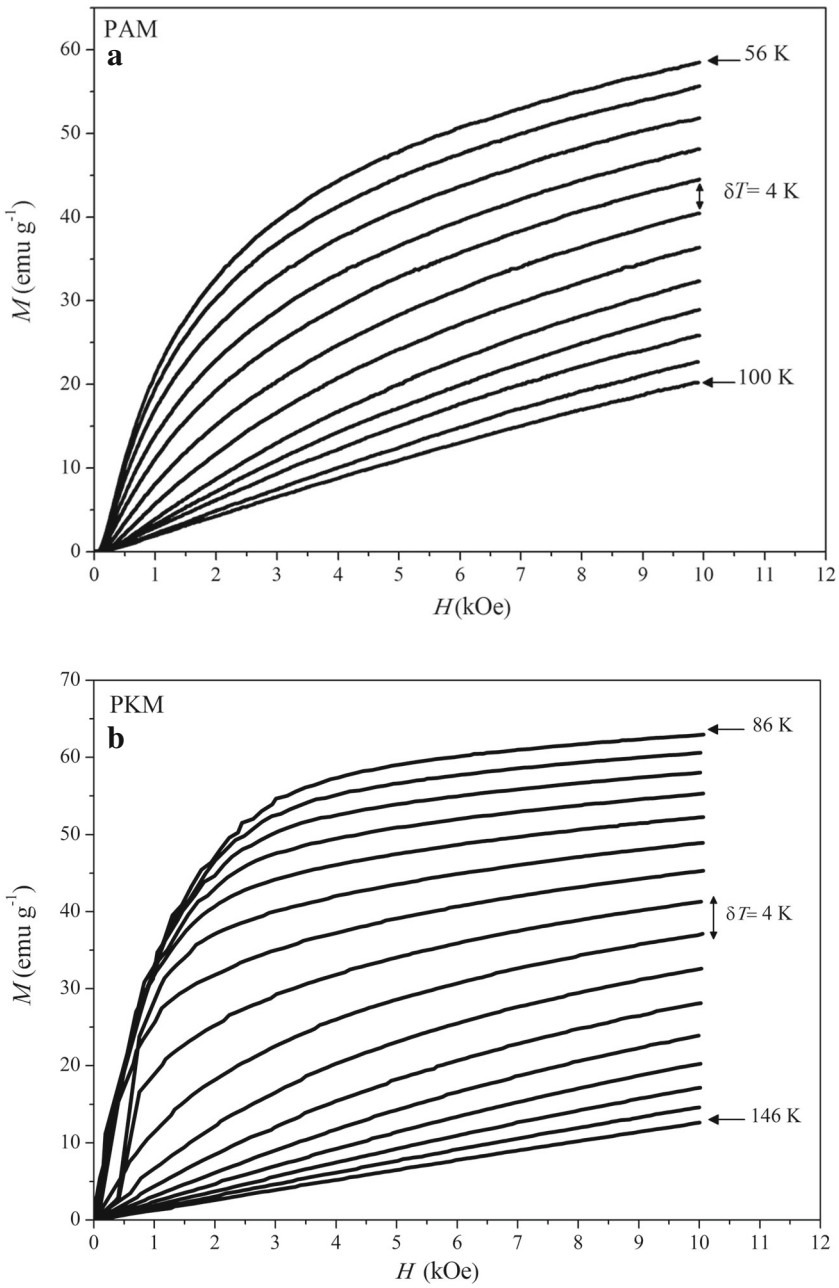

Fig. 4 $M(H)$ curves of the $Pr_{0.85}A_{0.15}MnO_3$ samples near T_C for **a** A = Ag and **b** A = K

where A, B, and C are the Landau coefficients. The Landau theory of ferromagnetism assumes that equilibrium condition around T_C so that the magnetic free energy can be minimized. From the minimization, $\frac{\partial G(M,T)}{\partial M} = 0$, a magnetic equation of state is obtained as

$$\frac{H}{M} = A(T) + B(T)M^2 + C(T)M^4 \tag{3}$$

The corresponding magnetic entropy change is obtained from differentiation of the magnetic part of the free energy with respect to the temperature

$$-\Delta S_M = \left(\frac{\partial G}{\partial T}\right)_H = \frac{1}{2}A'(T)M^2 + \frac{1}{4}B'(T)M^4 + \frac{1}{6}C'(T)M^6 \tag{4}$$

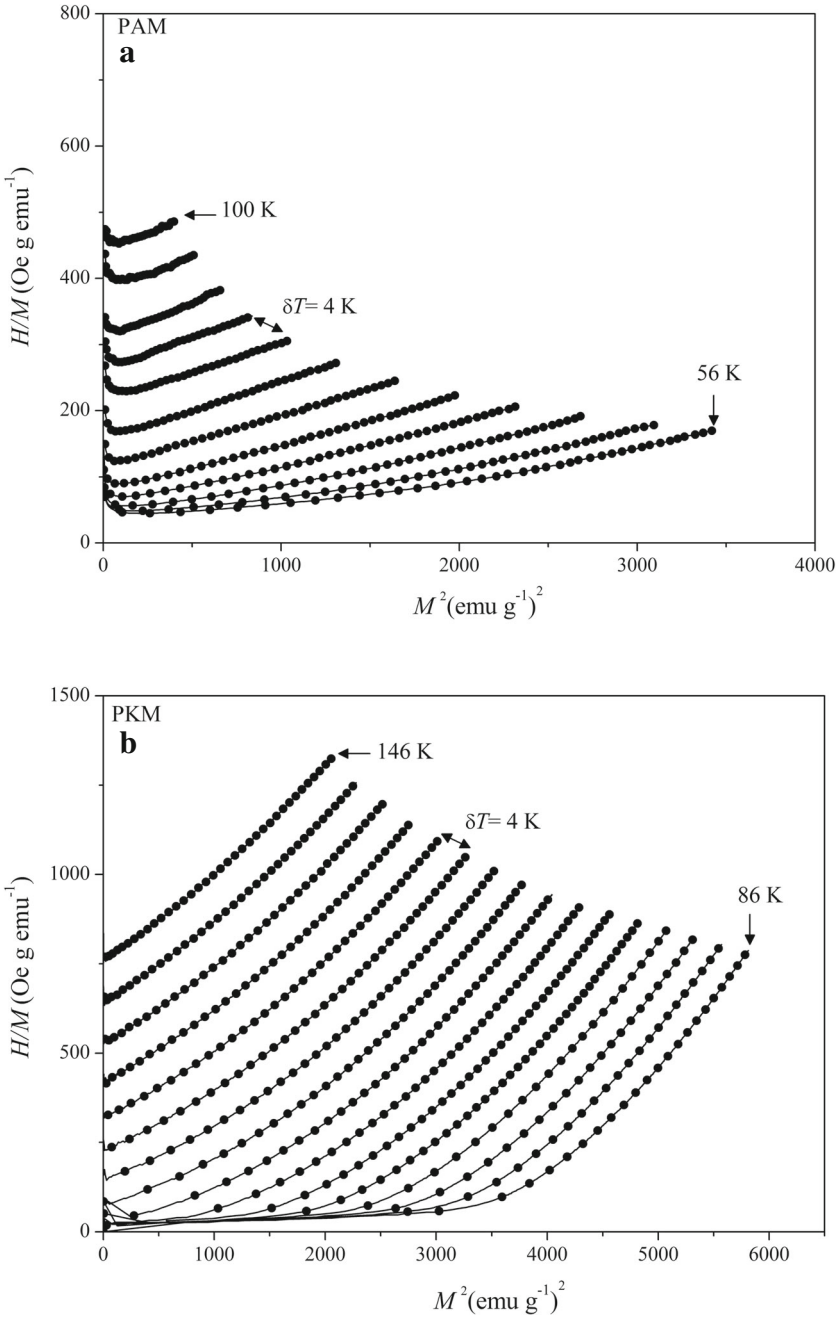

Fig. 5 The Arrott plots of the $Pr_{0.85}A_{0.15}MnO_3$ samples near T_C for **a** A = Ag and **b** A = K

where $A'(T)$, $B'(T)$, and $C'(T)$ are the temperature derivatives of the expansion coefficients. Using these values, we have calculated the temperature dependence of magnetic entropy change in an applied external magnetic field of 1 T of the samples. Figure 7 shows the temperature dependence of magnetic entropy change curves for both samples. It is seen from Fig. 7 that the magnetic entropy change curve calculated by the Landau theory is consistent with experimental curve. From this result and the theory explained above, it can be concluded that both the magnetoelastic coupling and the electron condensation energy play an important role on the MCE properties in our samples [45, 46].

The relative cooling power (RCP), which is related to the amount of heat transfer between cold and hot parts of

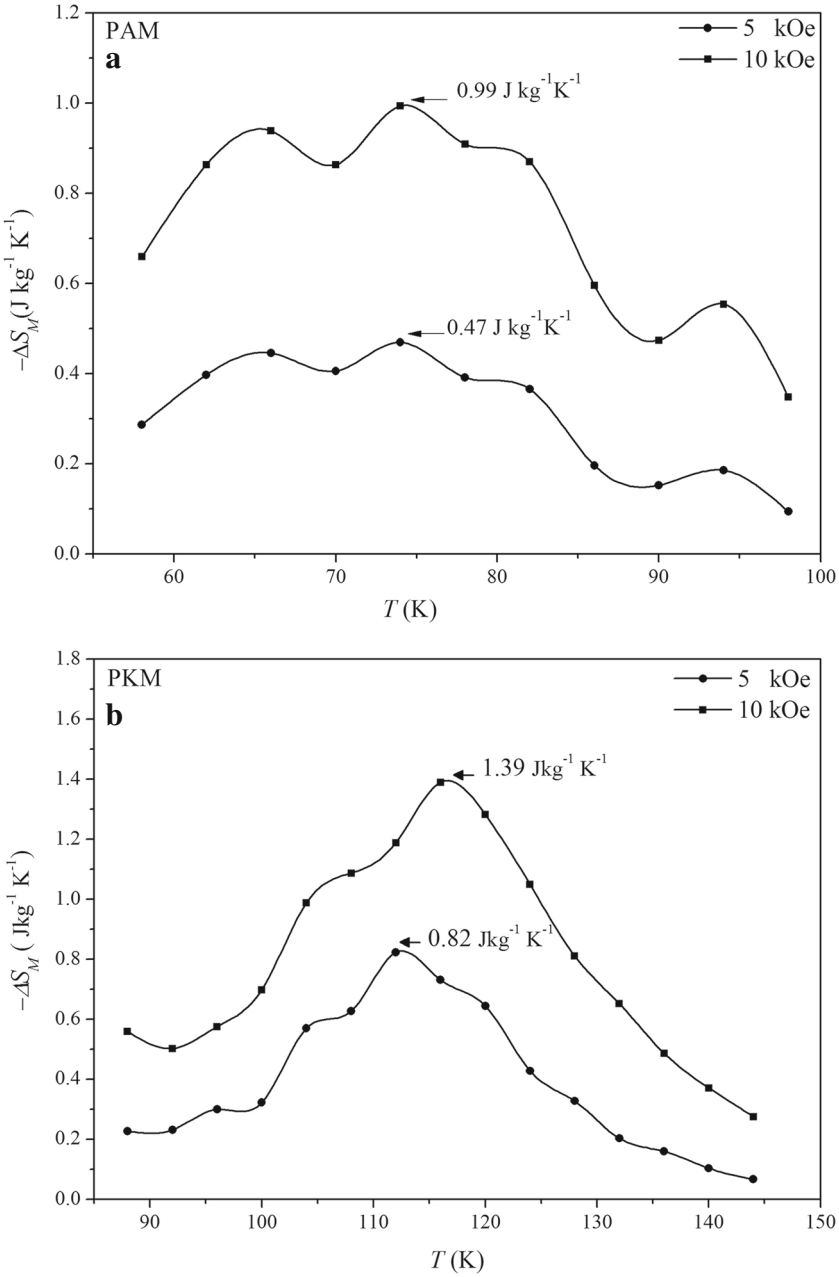

Fig. 6 The temperature dependence of ΔS_M for the $Pr_{0.85}A_{0.15}MnO_3$ samples at 5 and 10 kOe magnetic fields for **a** A = Ag and **b** A = K

refrigerator in an ideal thermodynamic cycle [47], is an important parameter in determining the efficiency of cooling. The RCP is defined as [48]

$$\mathrm{RCP} = \left|-\Delta S_{\mathrm{M}}^{\max}\right| \times \delta T_{\mathrm{FWHM}} \tag{5}$$

where $\left|-\Delta S_{\mathrm{M}}^{\max}\right|$ is the absolute value of maximum magnetic entropy change and δT_{FWHM} is the full width at half maximum of the magnetic entropy change curve. The RCP values of the samples were determined from Fig. 6a, b. Although the $-\Delta S_{\mathrm{M}}^{\max}$ value of the PKM is higher than that of the PAM, its RCP value (33.7 J kg^{-1}) is lower than that of PAM (35.6 J kg^{-1}) at the same magnetic field change. This situation results from the broadening of the $\Delta S_{\mathrm{M}}^{\max}$ curve which yields to increase the applicability of the magnetic cooling materials [49].

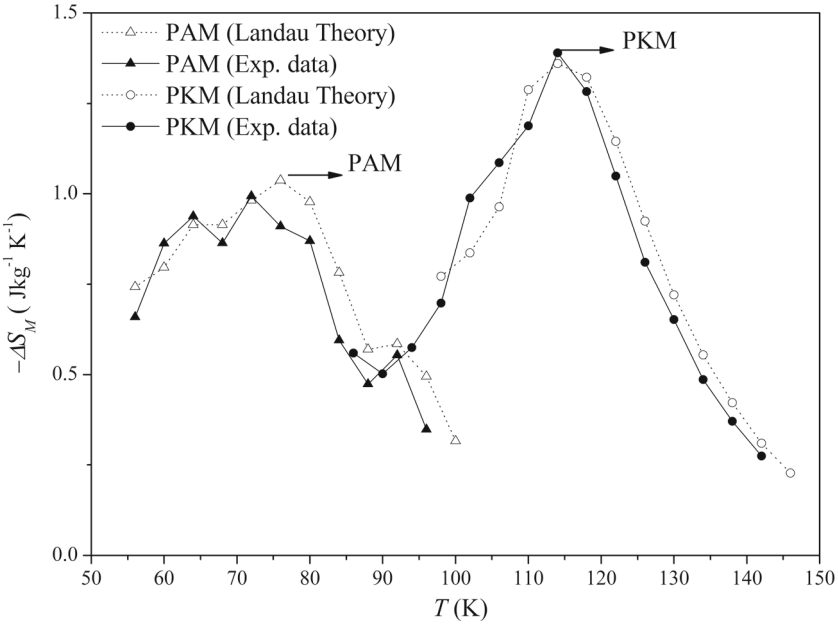

Fig. 7 The temperature dependence of magnetic entropy changes for the PKM and PAM samples under a magnetic field of 1 T. The theoretical calculations by using the Landau theory are fitting with the experimental data

4 Conclusions

We have investigated the influence of monovalent element doping on structural, magnetic, and magnetocaloric properties of $Pr_{0.85}A_{0.15}MnO_3$ (A = Ag and K) polycrystalline samples. The X-ray powder diffraction analysis reveals that the PAM and PKM samples have orthorhombic structure. The unit cell volumes and the lattice parameters vary monotonically with the $\langle r_A \rangle$. The ferromagnetic-to-paramagnetic phase transition temperature increases with increasing the $\langle r_A \rangle$. It is assumed that increasing $\langle r_A \rangle$ leads to an increase of double-exchange interaction. Both samples show second-order magnetic phase transition nature. The maximum magnetic entropy changes were determined as 0.99 and 1.39 J kg^{-1} K^{-1} for PAM and PKM samples for a field change of 1 T, respectively. Under the same magnetic field change, the RCP value of the PAM sample is bigger than that of the PKM due to having a broader magnetic phase transition of the PAM sample. As explained above, the obtained values are comparable to magnetocaloric Pr-based manganites.

Acknowledgments This work is supported by the Research Fund of Adıyaman University, Adıyaman, Turkey, under grant contract no. FEFBAP/2014-0008 and the Research Fund of Çukurova University, Adana, Turkey, under grant contract nos. FBA-2015-5028 and FEF2012D12.

References

1. Tozri, A., Khelifi, J., Dhahri, E., Hlil, E.K.: Influence of Pr-doping on magnetic phase transition and magnetocaloric effect of $La_{0.7-x}Pr_xBa_{0.3}MnO_3$ manganite. Mater. Chem. Phys. **149-150**, 728–733 (2015)
2. Mahaton, R.N., Sethupathi, K., Sankaranarayanan, V., Nirmala, R.: Co-existence of giant magnetoresistance and large magnetocaloric effect near room temperature in nanocrystalline $La_{0.7}Te_{0.3}MnO_3$. J. Magn. Magn. Mater. **322**, 2537–2540 (2010)
3. Xu, Y., Meier, M., Das, P., Koblischka, M.R., Hartmann, U.: Perovskite manganites: Potential materials for magnetic cooling at or near room temperature. Cryst. Eng. **5**, 383–389 (2002)
4. Zimm, C.B., Jastrab, A., Sternberg, A., Pecharsky, V.K., Gschneidner Jr., K.A., Osborne, M., Anderson, I.: Description and Performance of a Near-Room Temperature Magnetic Refrigerator. Adv. Cryog. Eng. **43**, 1759–1766 (1998)
5. Das, S., Dey, T.K.: Magnetic entropy change in polycrystalline $La_{1-x}K_xMnO_3$ perovskites. J. Alloys Compd. **440**, 30–35 (2007)
6. Das, S., Dey, T.K.: Above room temperature magnetocaloric properties of $La_{0.7}Ba_{0.3-z}Na_zMnO_3$ compounds. Mater. Chem. Phys. **108**, 220–226 (2008)
7. Cherif, R., Hlil, E.K., Ellouze, M., Elhalouani, F., Obbade, S.: Magnetic and magnetocaloric properties of $La_{0.6}Pr_{0.1}Sr_{0.3}Mn_{1-x}Fe_xO_3$ ($0 \leq x \leq 0.3$) manganites. J. Solid Stat. Chem. **215**, 271–276 (2014)
8. Dan'kov, S.Y., Tishin, A.M., Pecharsky, V.K., Gschneidner, K.A.: Magnetic phase transitions and the magnetothermal properties of gadolinium. Phys. Rev. B **57**, 3478–3490 (1998)
9. Pan, M.H., Yu, S.C., Hur, N.H.: Excellent magnetocaloric properties of $La_{0.7}Ca_{0.3-x}Na_xMnO_3$ $0.05 \leq x \leq 0.25$ single crystals. Appl. Phys. Lett. **86**, 072504-3 (2005)

10. Anwar, M.S., Ahmed, F., Koo, B.H.: Structural distortion effect on the magnetization and magnetocaloric effect in Pr modified $La_{0.65}Sr_{0.35}MnO_3$ manganite. J. Alloys Compd. **617**, 893–898 (2014)
11. Cheikh-Rouhou Koubaa, W., Koubaa, M., Cheikhrouhou, A.: Effect of potassium doping on the structural, magnetic and magnetocaloric properties of $La_{0.7}Sr_{0.3-x}K_xMnO_3$ perovskite manganites. J. Alloys Compd. **470**, 42–46 (2009)
12. Çetin, S.K., Acet, M., Ekicibil, A., Sarıkürkçü, C., Kıymaç, K.: Reversibility in the adiabatic temperature change of $Pr_{0.73}Pb_{0.27}MnO_3$. J. Alloys Compd. **565**, 139–143 (2013)
13. Ur. Rehman, Z., Anwar, M.S., Koo, B.H.: Influence of Barium Doping on the Magnetic and Magnetocaloric Properties of $Pr_{1-x}Ba_xMnO_3$. J. Supercond. Nov. Magn. **28**, 1629–1634 (2015)
14. Righi, L., Gorria, P., Insausti, M., Gutiérrez, J., Barandiaran, J.M.: Influence of Fe in giant magnetoresistance ratio and magnetic properties of $La_{0.7}Ca_{0.3}Mn_{1-x}Fe_xO_3$ perovskite type compounds. J. Appl. Phys. **81**, 5767–5769 (1997)
15. Maignan, A., Damay, F., Martin, C., Raveau, B.: Nickel-induced metal-insulator transition in the small a cation manganites $Ln_{0.5}Ca_{0.5}MnO_3$. Mater. Res. Bull. **32**, 965–972 (1997)
16. Jirák, Z., Hejtmánek, J., Knízek, K., Sonntag, R.: Structure and properties of the $Pr_{1-x}K_xMnO_3$ perovskites ($x = 0 - 0.15$). J. Solid Stat. Chem. **132**, 98–106 (1997)
17. Jirák, Z., Hejtmánek, J., Knízek, K., Maryško, M., Pollert, E., Dlouhá, M., Vrastislav, S., Kužel, R., Hervieu, M.: Structure and magnetism in the $Pr_{1-x}Na_xMnO_3$ perovskites ($0 \leq x \leq 0.2$). J. Magn. Magn. Mater. **250**, 275–287 (2002)
18. Zouari, S., Cheikh-Rouhou, A., Strobel, P., Pernet, M., Pierre, J.: Structural and magnetic properties of alkali-substituted praseodymium manganites $Pr_{1-x}A_xMnO_3$ (A = Na, K). J. Alloys Compd. **333**, 21–27 (2002)
19. Thaljaoui, R., Boujelben, W., Pękała, M., Pękała, K., Fagnard, J.-F., Vanderbemden, P., Donten, M., Cheikhrouhou, A.: Magnetocaloric effect of monovalent K doped manganites $Pr_{0.6}Sr_{0.4-x}K_xMnO_3$ (x = 0 to 0.2). J. Magn. Magn. Mater. **352**, 6–12 (2014)
20. Reis, M.S., Amaral, V.S., Araújo, J.P., Tavares, P.B., Gomes, A.M., Oliveira, I.S.: Magnetic entropy change of $Pr_{1-x}Ca_xMnO_3$ manganites ($0.2 \leqslant x \leqslant 0.95$). Phys. Rev. B **71**, 144413–144418 (2005)
21. Chen, P., Du, Y.W., Ni, G.: Low-field magnetocaloric effect in $Pr_{0.5}Sr_{0.5}MnO_3$. Europhys. Lett. **52**, 589–593 (2000)
22. Alonso, J.A., Casais, M.T., Martinez-Lope, M.J., Martinez, J.L., Fernandez-Diaz, M.T.: A structural study from neutron diffraction data and magnetic properties of RMn2O5 (R = La, rare earth). J. Phys. Condens. Matter **9**, 8515–8526 (1997)
23. Shindea, K.P., Deshpande, N.G., Eom, T., Lee, Y.P., Pawara, S.H.: Solution-combustion synthesis of $La_{0.65}Sr_{0.35}MnO_3$ and the magnetocaloric properties. Mater. Sci. Eng. B **167**, 202–205 (2010)
24. Shannon, R.D.: Revised effective ionic radii and systematic studies of interatomic distances in halides and chalcogenides. Acta Crystallogr. Sect. A **32**, 751–767 (1976)
25. Ahmed, A.M., Papavassiliou, G., Mohamed, H.F., Ibrahim, E.M.M.: Structural, magnetic and electronic properties on the Li-doped manganites. J. Magn. Magn. Mater. **392**, 27–41 (2015)
26. Thaljaoui, R., Boujelben, W., Pękała, M., Pociecha, D., Syzdłowska, J., Cheikhrouhou, A.: Room temperature magnetocaloric and magneto-transport properties of monovalent doped $Pr_{0.6}Sr_{0.35}Na_{0.05}MnO_3$ manganite. J. Alloys Compd. **530**, 138–143 (2012)
27. Das, S., Dey, T.K.: Structural and magnetocaloric properties of $La_{1-y}Na_yMnO_3$ compounds prepared by microwave processing. J. Phys. D: Appl. Phys. **40**, 1855–1863 (2007)
28. Bohigas, X., Tejada, J., Del Barco, E., Zhang, X.X., Sales, M.: Tunable magnetocaloric effect in ceramic perovskites. Appl. Phys. Lett. **73**, 390–392 (1998)
29. Ho, T.A., Dang, N.T., Phan, T.L., Yang, D.S., Lee, B.W., Yu, S.C.: Magnetic and magnetocaloric properties in $La_{0.7}Ca_{0.3-x}Na_xMnO_3$ exhibiting first-order and secondorder magnetic phase transitions. J. Alloys Compd. (2016) doi:10.1016/j.jallcom.2016.03.156
30. Nam, D.N.H., Mathieu, R., Nordblad, P., Khiem, N.V., Phuc, N.X.: Ferromagnetism and frustration in $Nd_{0.7}Sr_{0.3}MnO_3$. Phys. Rev. B **62**, 1027 (2000)
31. Freitas, R.S., Ghivelder, L., Damay, F., Dias, F., Cohen, L.F.: Magnetic relaxation phenomena and cluster glass properties of $La_{0.7-x}Y_xCa_{0.3}MnO_3$ manganites. Phys. Rev. B **64**, 144404 (2001)
32. Radaelli, P.G., Iannone, G., Marezio, M., Hwang, H.Y., Cheong, S.-W., Jorgensen, J.D., Argyriou, D.N.: Structural effects on the magnetic and transport properties of perovskite $A_{1-x}A'_xMnO_3$ ($x = 0.25, 0.30$). Phys. Rev. B **56**, 8265–8276 (1997)
33. Anwar, M.S., Kumar, S., Ahmed, F., Heo, S.N., Kim, G.W., Koo, B.H.: Study of magnetic entropy change in $La_{0.65}Sr_{0.35}Cu_{0.1}Mn_{0.9}O_3$ complex perovskite. J. Electroceramics **30**, 46–50 (2013)
34. Mtiraoui, N., Dhahri, J., Oumezine, M., Dhahri, E.: Magnetic and Magnetocaloric Properties of $La_{0.67}Pb_{0.33-x}Ag_xMnO_3$ Compounds. Supercond. Nov. Magn. **25**, 1937–1945 (2012)
35. Raju, K., Pavan Kumar, N.P., Venugopal Reddy, P.V., Yoon, D.H.: Influence of Eu doping on magnetocaloric behavior of $La_{0.67}Sr_{0.33}MnO_3$. Phys. Lett. A. **379**, 1178–1182 (2015)
36. Ayas, A.O., Akyol, M., Cetin, S.K., Akca, G., Ekicibil, A., Ozcelik, B.: Magnetocaloric Properties of $La_{0.85}Ag_{0.15}MnO_3$ and $(La_{0.80}Pr_{0.20})_{0.85}Ag_{0.15}MnO_3$ Compounds. J. Supercond. Nov. Magn. **28**, 1649–1658 (2015)
37. Ayas, A.O., Akyol, M., Ekicibil, A.: Structural and magnetic properties with large reversible magnetocaloric effect in $(La_{1-x}Pr_x)_{0.85}Ag_{0.15}MnO_3$ ($0.0 \leq x \leq 0.5$) compounds. Philos. Mag. **96**, 922–937 (2016)
38. Bebenin, N.G., Zainullina, R.I., Ustinov, V.V., Mukovskii, Y.M.: Magnetic properties of $La_{0.7-x}Pr_xCa_{0.3}MnO_3$ single crystals: When is Banerjee criterion applicable? J. Magn. Magn. Mater. **354**, 76–80 (2014)
39. Banerjee, S.K.: On a generalised approach to first and second order magnetic transitions. Phys. Lett. **12**, 16–17 (1964)
40. Foldeaki, M., Chahine, R., Bose, T.K.: Magnetic measurements: A powerful tool in magnetic refrigerator design. J. Appl. Phys. **77**, 3528–3537 (1995)
41. Zhang, P., Yang, H., Zhang, S., Ge, H., Pan, M.: Effect of Li doping on the magnetic and magnetocaloric properties of $Pr_{0.5}Sr_{0.5-x}Li_xMnO_3$ ($0 \leq x \leq 0.3$). J. Magn. Magn. Mater. **334**, 16–20 (2013)
42. Suemitsu, M., Nakagawa, T., Hirayama, Y., Seino, S., Yamamoto, T.A.: Magnetocaloric effect of $La_{0.7-x}Pr_xCa_{0.3}MnO_3$ perovskites. J. Alloys Compd. **551**, 195–199 (2013)
43. Amaral, J.S., Reis, M.S., Amaral, V.S., Mendonça, T.M., Araújo, J.P., Tavares, P.B., Vieira, J.M.: Magnetocaloric effect in Er- and Eu-substituted ferromagnetic La-Sr manganites. J. Magn. Magn. Mater. **290–291**, 686–689 (2005)
44. Amaral, V.S., Amaral, J.S.: Magnetoelastic coupling influence on the magnetocaloric effect in ferromagnetic materials. J. Magn. Magn. Mater. **272**, 2104–2105 (2004)
45. Anwar, M.S., Kumar, S., Ahmed, F., Arshi, N., Kim, G.W., Koo, B.H.: Above room temperature magnetic transition and magnetocaloric effect in $La_{0.66}Sr_{0.34}MnO_3$. J. Korean Physical Society **60**, 1587–1592 (2012)

46. Varvescu, A., Deac, I.G.: Critical magnetic behavior and large magnetocaloric effect in $Pr_{0.67}Ba_{0.33}MnO_3$ perovskite manganite. Physica B **470-471**, 96–101 (2015)
47. Tishin, A.M., Spichkin, Y.I.: The magnetocaloric effect and its applications. Institute of Physics Publishing, Bristol, UK (2003)
48. Gschneidner, K.A., Pecharsky, V.K.: Magnetocaloric Materials. Annu. Rev. Mater. Sci. **30**, 387–429 (2000)
49. Debnath, J.C., Zeng, R., Kim, J.H., Dou, S.X.: Improvement of refrigerant capacity of $La_{0.7}Ca_{0.3}MnO_3$ material with a few percent Co doping. J. Magn. Magn. Mater. **323**, 138–143 (2011)